Remote Sensing

– Principle and applications in geology –

Isao SATO
Institute of Geology and Geoinformation,
Geological Survey of Japan, AIST

Abstract

In the training, I introduce basic principle and knowledge of remote sensing, which is related to geologic applications. Remote sensing is widely applied to geoscience, however, it is impossible to introduce all of them. You can overview the spectral features of geologic objects. In addition, several selected topics are introduced through our past research activities. These topics cover traditional geologic mapping and novel applications in geology, such as InSAR applications (DEM generation, deformation mapping), hyperspectral remote sensing, SAR polarimetry.

Remote Sensing

- Principle and applications in geology -

Isao SATO

Institute of Geology and Geoinformation

for APEC Training Material

My talks

- Overview of Remote Sensing in Geology
  - Physical background of 'remote sensing'
    - Optical region
    - Microwave region (SAR)
- Selective topics
  - Geologic structure and unit mapping
  - Volcano monitoring
  - Hyperspectral analysis
  - InSAR (Interferometric SAR technique)
  - SAR Polarimetry

One definition of 'remote sensing'

(there are variants in the literature.)

"***the observation of a target by a device separated from it by some distance thus without physical contact***"

target

In geology, natural targets (rocks, minerals, soils, terrain structures) over the Earth are observed. In general, all materials distributed over the surface are targets in remote sensing for various fields.

device

Optical, microwave, laser instruments are often used as device onboard cars, airplanes, satellites. Ground instrument is also used in the field work. Instruments are categorized into passive and active devices.

◆ *The advantage and limitation in remote sensing*

Merits of satellite observation

- Wide coverage
- Simultaneous observation over large area
- Repeatability

Limitations

- Most of instruments can observe physical parameters of very thin ground surface. Microwave instruments can penetrate very dry materials, but its penetration depth is about a few meters, which depends on surface moisture.
- Optical imagers can not observe any material under the cloud.

Global Observation mechanism

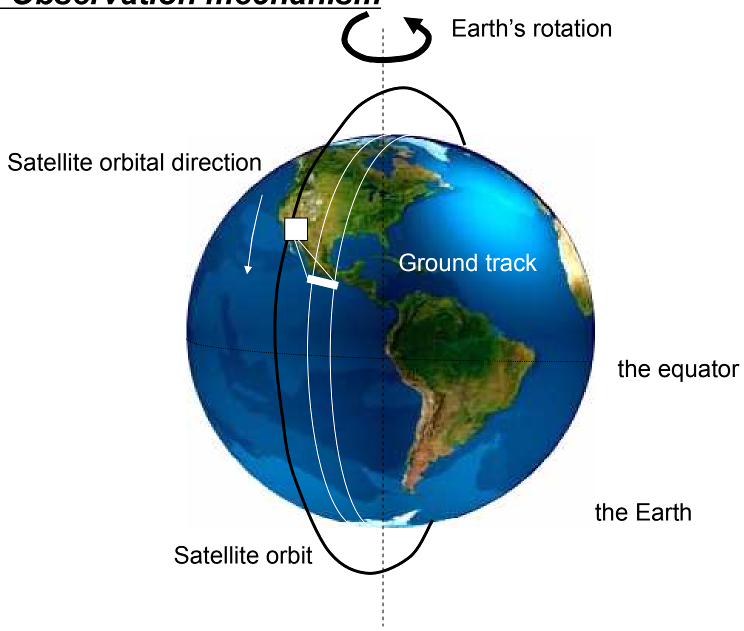

Observation from satellite

Instrument oriented to the Earth detects digital signals, which contains direct and diffused lights reflected at the surface, and diffused light in the atmosphere, through the telescope, A/D converter, detectors. Multi-spectral image can be obtained by using different wavelengths. Optical and microwave instruments have different observation geometry, as illustrated the bellow.

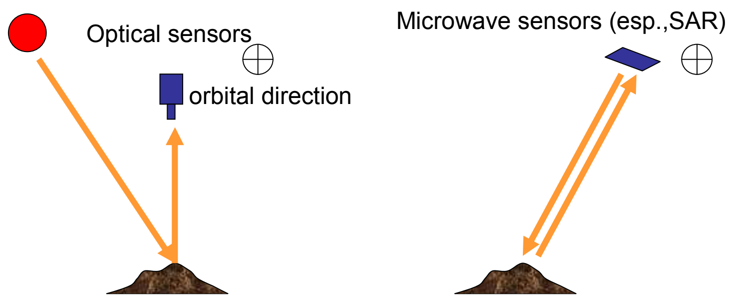

Mechanism of Optical remote sensing

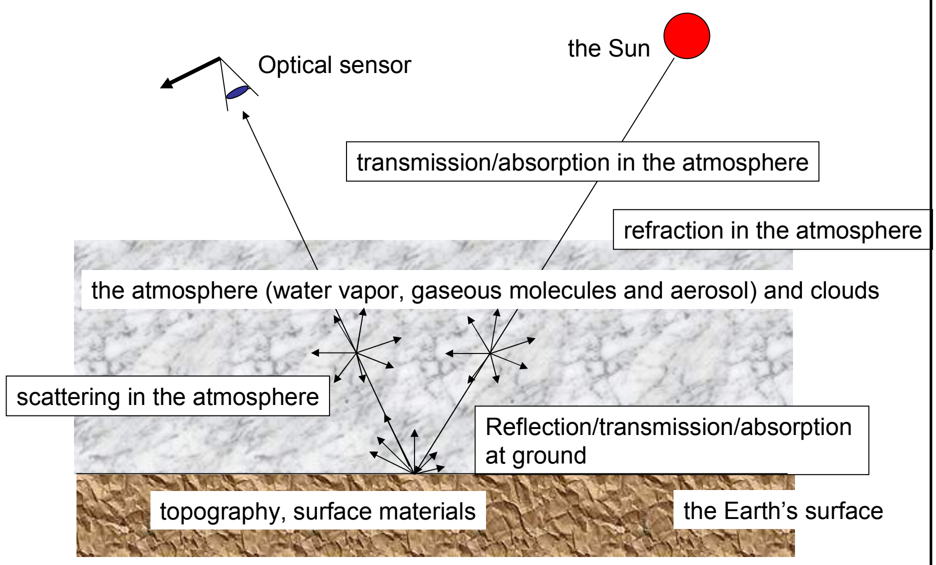

Wavelength region used in remote sensing

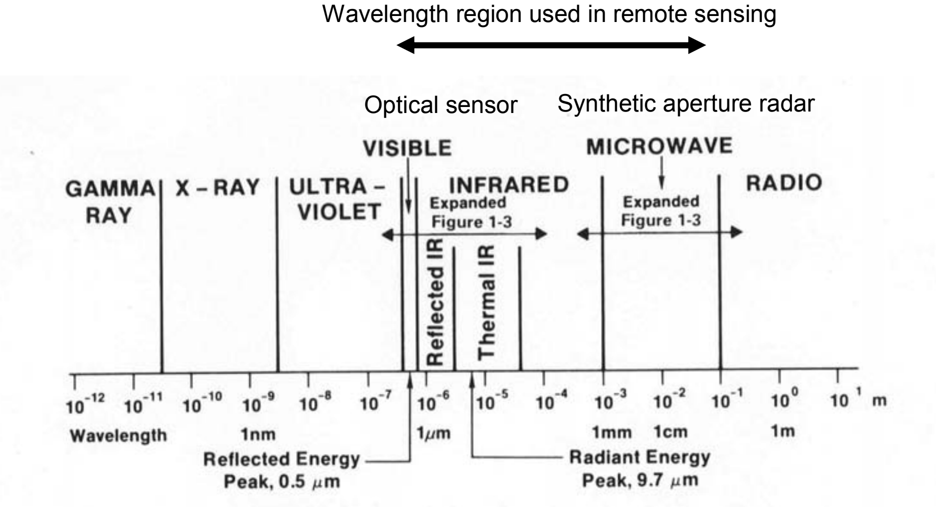

wavelength of electromagnetic wave

Interaction between the Sun and the Earth's surface

AIST

Sun's energy and radiant energy from materials

Planck's Eqn.

$$E_\lambda = B(\lambda, T) = \frac{c_1}{\lambda^5\left[\exp\left(c_2/\lambda T\right)-1\right]} \qquad T = \frac{c_2}{\lambda \ln\left(\frac{c_1}{\lambda^5 E_\lambda}\right)+1}$$

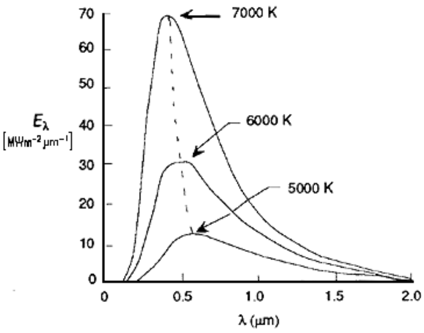

Blackbody radiation

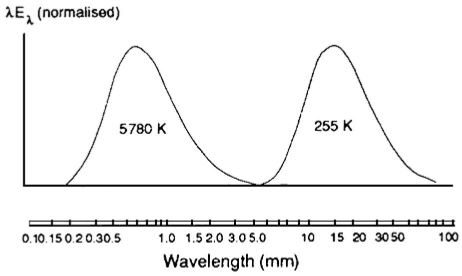

Normalized radiation

Atmospheric transmittance and atmospheric window

AIST

for optical sensor

'Atmospheric window' have been used for observation from space.

for SAR

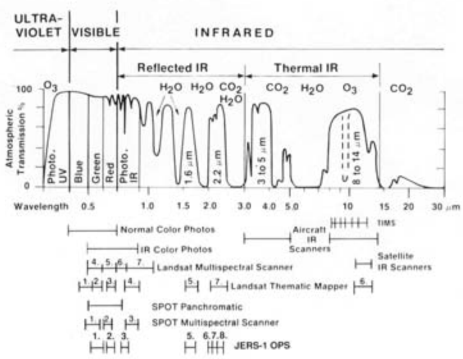

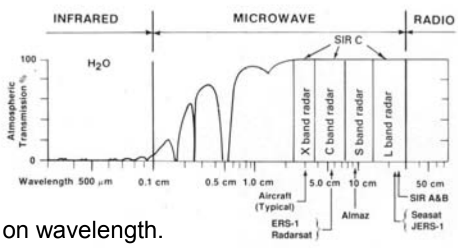

Atmospheric transmittance depends on wavelength.

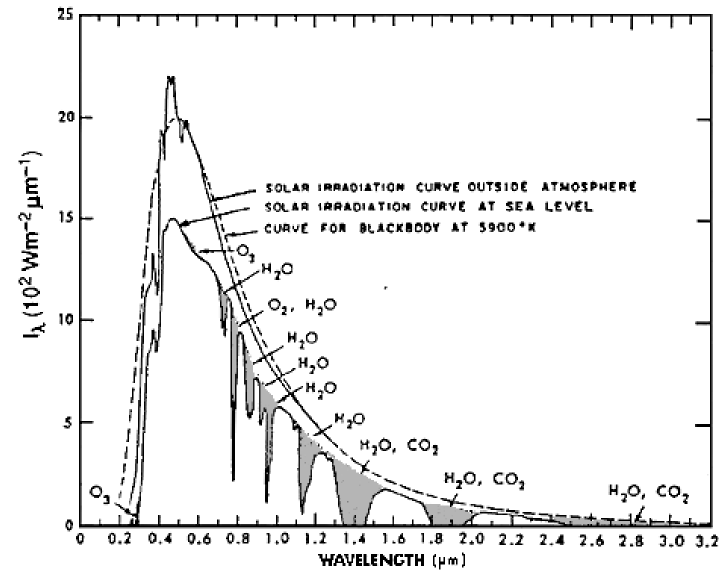

Spectral irradiance at the top of atmosphere and at sea level

NATIONAL INSTITUTE OF ADVANCED INDUSTRIAL SCIENCE AND TECHNOLOGY (AIST)

Reflectance and emissivity features of rocks and minerals

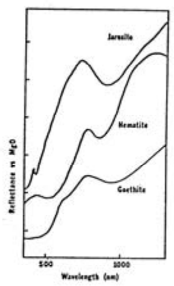

Visible and near-infrared spectra of iron-oxide minerals
(Hunt and AS=shlry/1979)

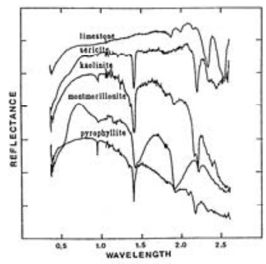

Shortwave infrared spectra of altered and carbonate minerals

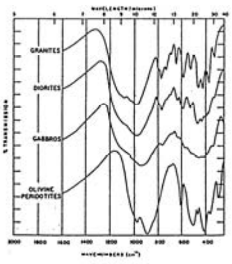

Thermal infrared spectra of igneous rocks
(Hunt,1980)

Spectral characteristics from visible to thermal infrared regions of typical rocks and minerals

NATIONAL INSTITUTE OF ADVANCED INDUSTRIAL SCIENCE AND TECHNOLOGY (AIST)

Absorption wavelength in VNIR region and its principle

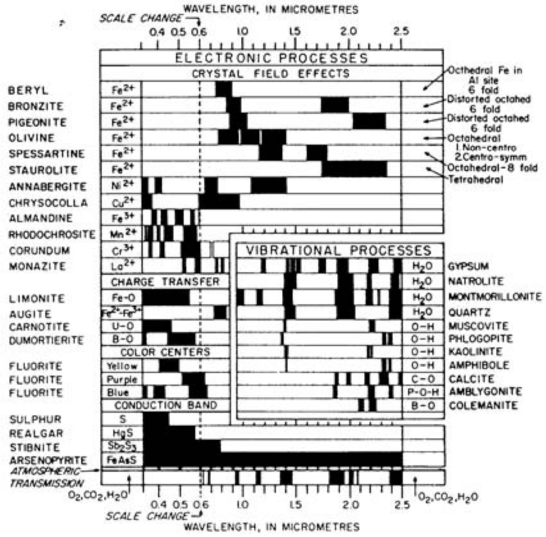

FIGURE 17. Composite diagram showing the location of the spectral features (wavelength of the center of black areas) and half-width (width of black areas) of most common minerals.*

Ref: Handbook of Physical Properties of Rocks

NATIONAL INSTITUTE OF ADVANCED INDUSTRIAL SCIENCE AND TECHNOLOGY (AIST)

Typical rocks and their emissivity characteristics in the thermal region

Absorbed wavelength (called as the Si-O reststrahlen band) in emissivity is systematically shifted to shorter wavelength, when the content of SiO2 is increased.

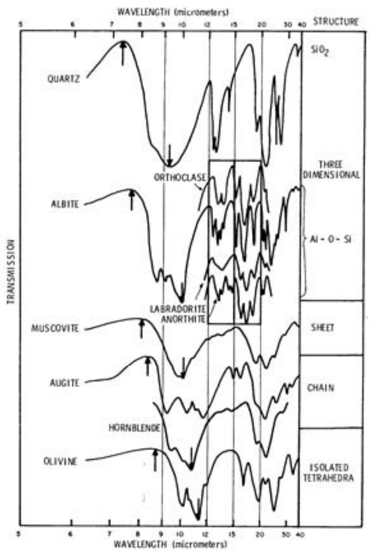

FIGURE 61. Transmission spectra of silicate minerals recorded in air. Five spectral regions are indicated and the causes of the features that occur there are discussed in the text.*

Ref: Handbook of Physical Properties of Rocks

NATIONAL INSTITUTE OF ADVANCED INDUSTRIAL SCIENCE AND TECHNOLOGY (AIST)

AIST

Spectral radiance, observed by the sensor

Radiative transfer function

$$L_\lambda(z) = T_\lambda \uparrow \cdot R_\lambda \cdot (E_{0\lambda} \cdot T_\lambda \downarrow \cdot \cos\theta + E_{a\lambda} \downarrow)/\pi + T_\lambda \uparrow \cdot \varepsilon_\lambda \cdot B_\lambda(Ts) + L_{p\lambda}(z)$$

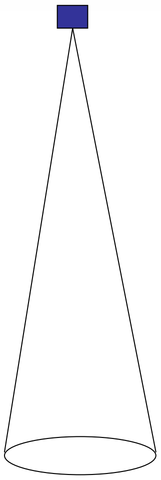

$L_\lambda(z)$: at-satellite spectral radiance at altitude z

$T_\lambda \uparrow$: upward atmospheric transmittance

$T_\lambda \downarrow$: downward atmospheric transmittance

R_λ : surface reflectance

ε_λ : surface emissivity

$E_{0\lambda}$: exatmospheric spectral irradiance

$E_{a\lambda} \downarrow$: surface incident spectral irradiance, reflected, scattered and emitted from the atmosphere

$B_\lambda(Ts)$: emission from the blackbody of temperature Ts

Ts : surface temperature

θ : sun zenith angle

$L_{p\lambda}(z)$: upward spectral radiance from the atmosphere at altitude z

AIST

Example

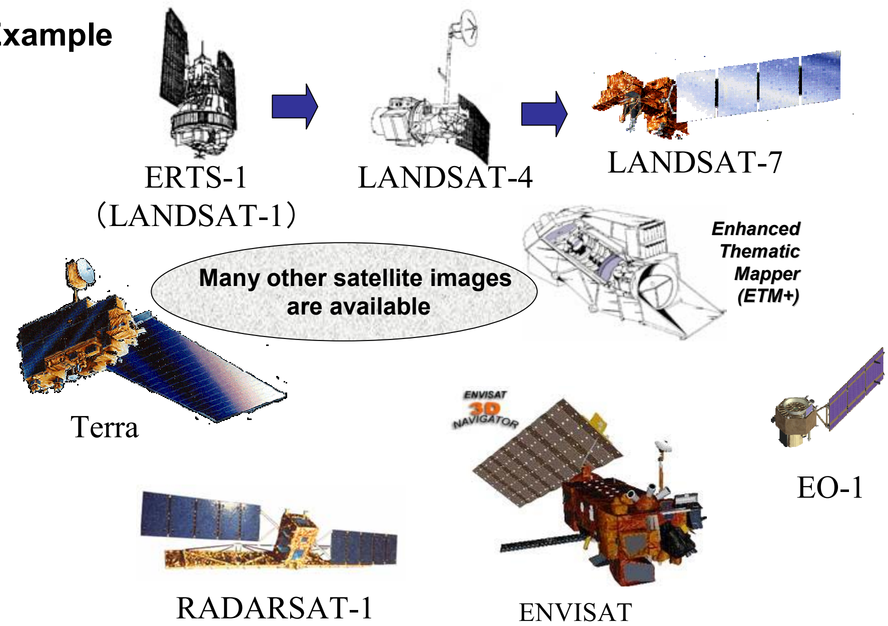

Observation bands of major optical sensors

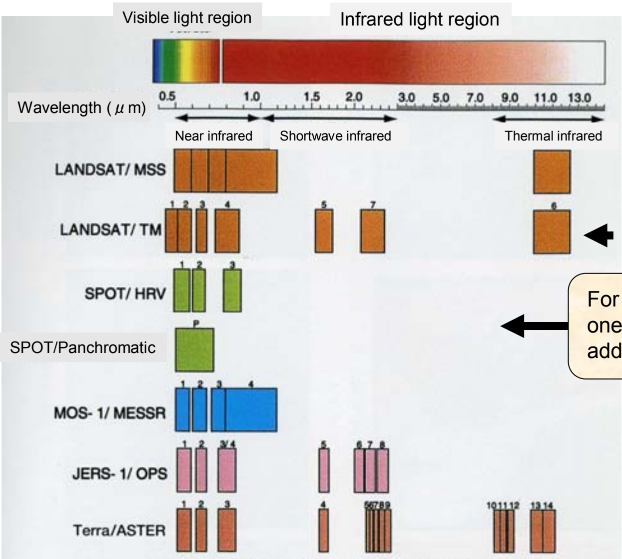

LANSAT7/ETM+

For SPOT5/HRVIR, one SWIR band is added.

Japan

Courtesy of ERSDAC

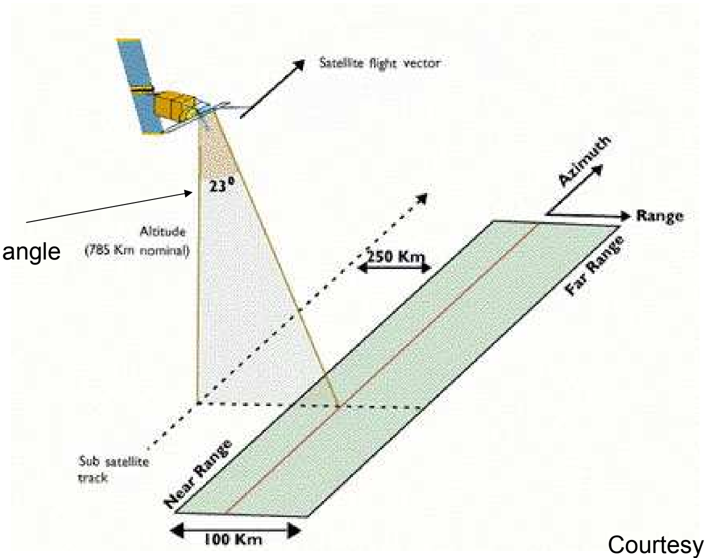

Off-nadir angle

Swath width

Courtesy of ESA

Observing geometry of SAR (in the case of AMI, onboard ESA's ERS satellite)

Geometric distortion of SAR observation

In SAR image, observed signal is imaged by slant range distance. Therefore, observed terrain is shifted to the sensor direction. Thus, it is required DEM data, when you make orthographic image of SAR.

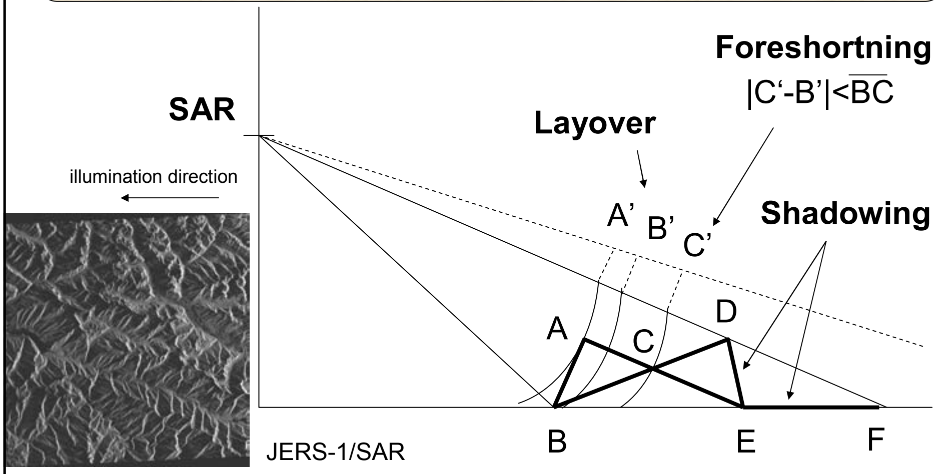

Relationship between incident angle and backscatter coefficient (which corresponds to the intensity of returned signal to the sensor) is affected by wavelength and roughness in SAR.

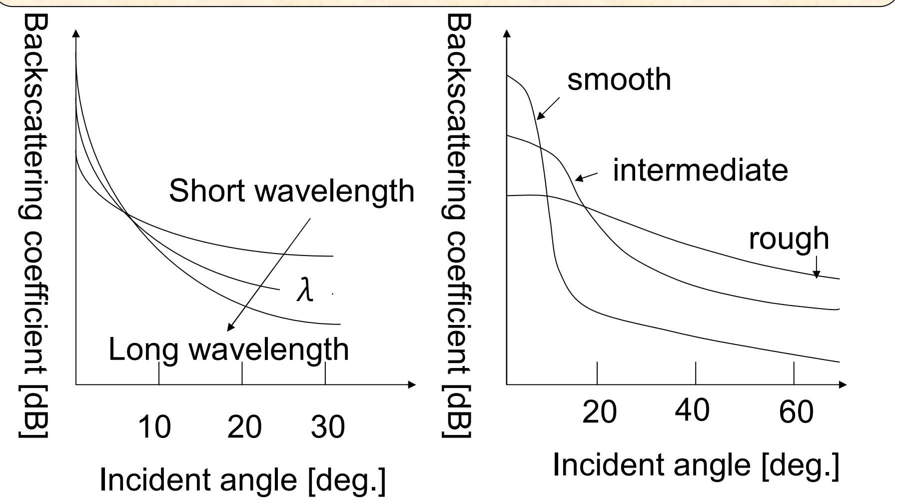

Radar scattering

1) smooth surface

2) ragged terrain surface

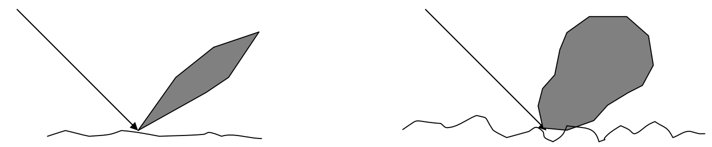

A criteria of smoothness (Rayleigh criteria)

$$\Delta h < (\lambda / 8 \cdot \cos\theta)$$

where, Δh is standard deviation of surface roughness, λ is wavelength, θ is incident angle.

Image display (Noise reduction)

Speckle reduction for SIR-C data (L-HH polarization)

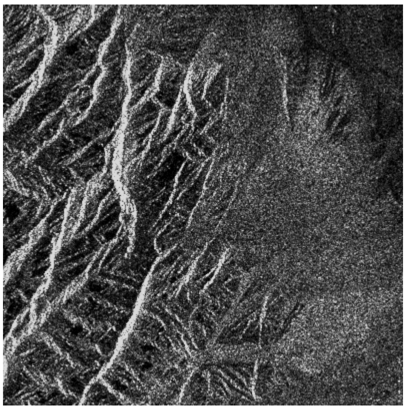

Original image

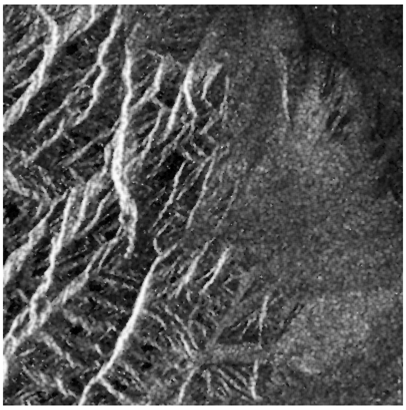

Filtered image by 3x3 Gamma filtering

There are several filters for speckle reduction.

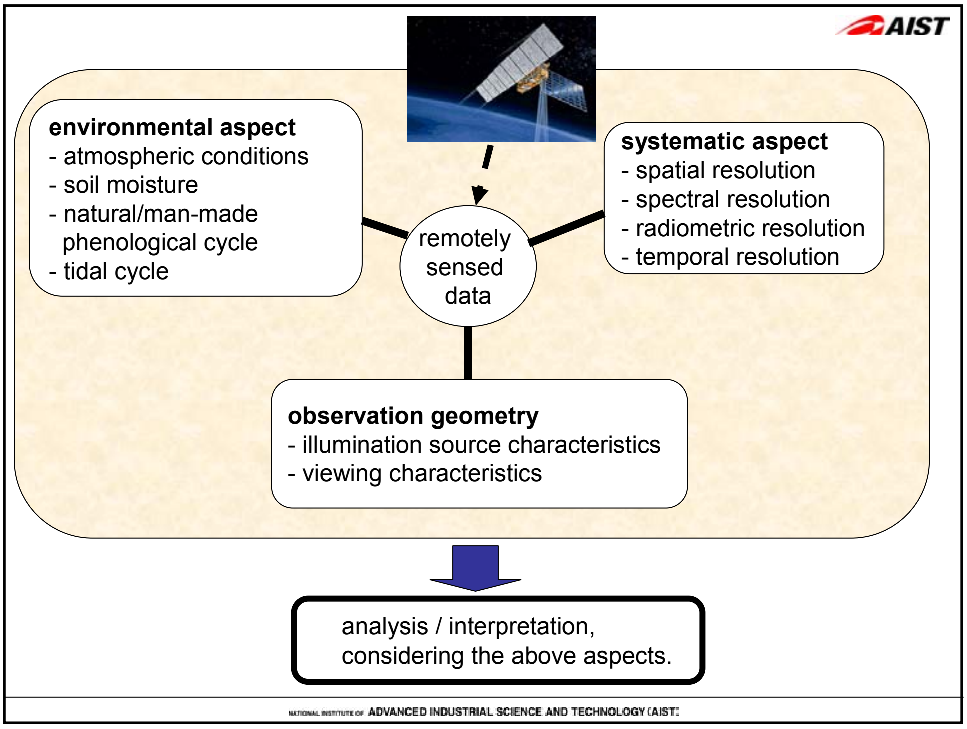

Overview of Remote Sensing in Geology

◆ ***Current trends on remote sensing (selective)***

- from qualitative to quantitative
  the calibrated and validated data is handled

- the increase of resolution (or data volume), but lower cost
  the highest spatial resolution is less than 1 m.
  the highest spectral resolution is more than 200 chs.

- the sophisticated multi-sensor analysis
  data fusion

- the availability of numerous and variety of data
  Landsat, SPOT, ALOS, Terra, Aqua, Radarsat, IRS, FORMOSAT, KOMPSAT, IKONOS, QuickBird, EO-1, ･････ (excluding airborne data)

NATIONAL INSTITUTE OF ADVANCED INDUSTRIAL SCIENCE AND TECHNOLOGY (AIST)

Overview of Remote Sensing in Geology

AIST

◆ Brief overview of remote sensing in geology

Remote sensing is widely used in a variety of applications relevant to geoscience since 1970s.

For example, remote sensing data have been used in:

- Mineral and petroleum exploration,
- Mapping geology, and geomorphology,
- Monitoring disasters (volcano eruptions, earthquake, land subsidence, and others), and
- Geologic environmental investigation

NATIONAL INSTITUTE OF ADVANCED INDUSTRIAL SCIENCE AND TECHNOLOGY (AIST)

Geologic Remote Sensing Research Group

AIST

The group will take a major role for creating geo-scientific information and knowledge from remotely sensed images, promoting effective use of the land and natural resources, and mitigating geo-hazards.

The **second mid-range research (2005 – 2009)**

- **Geo-information products development**
- **Geo-information infrastructure**
  - ***Satellite Image DB of active volcanoes**
- **Others**
  - ***Geology-related applications of Terra/ASTER and ALOS/PALSAR images**
  - ***Environmental research**

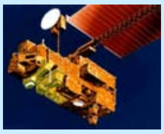

Terra Satellite and ASTER instrument

ALOS satellite and PALSAR instrument

JERS-1 Satellite

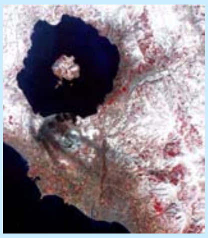

ASTER image after the eruption

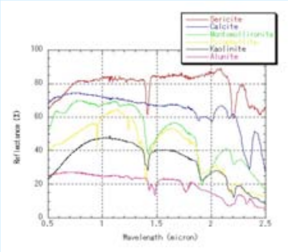

Spectra of typical clay minerals

Bird-view of Satuma-io-jima

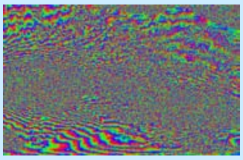

InSAR fringe after Izmit earthquake in Turkey

Spectra database of rocks/minerals

Reflectance spectra of typical minerals at laboratory is fundamental information for analyzing optical images for geology

- powder samples
- chemical analysis
- X-ray analysis

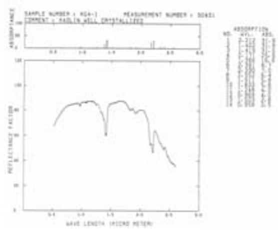

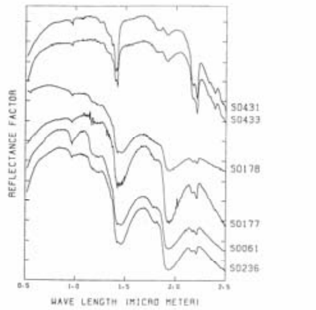

In-site spectra
→ coating effects
→ atmospheric effect

sam.Sample_ID	sam.Site	lab.Measurement_ID	norm.Kaolinite
KGa-1	Washington County	S0431	90.92000
KGa-2	Warren County	S0433	90.58000
860819F2	Goshogake	S0178	71.25000
860819F1	Fukenoyu	S0177	70.59000
851021-T1	Goshogake	S0061	64.00000
870216-S5	Komatsu-jigoku	S0236	62.46000

Reflectance spectra of kaolinite, measured at laboratory.

Vicarious Calibration for ASTER Instrument

Instrument calibration is monitored and validated through this activity.

Reflectance and atmospheric measurements

Onboard Cal. data
Image data

Simulation

Ground validation experiments
In U.S.A.

Estimated Calibration Coefficients

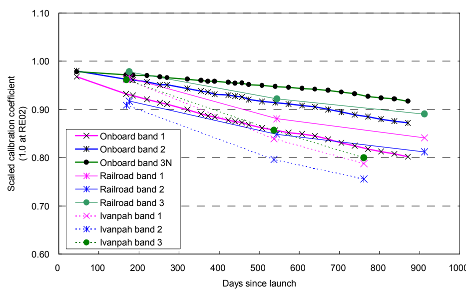

TIME after launch

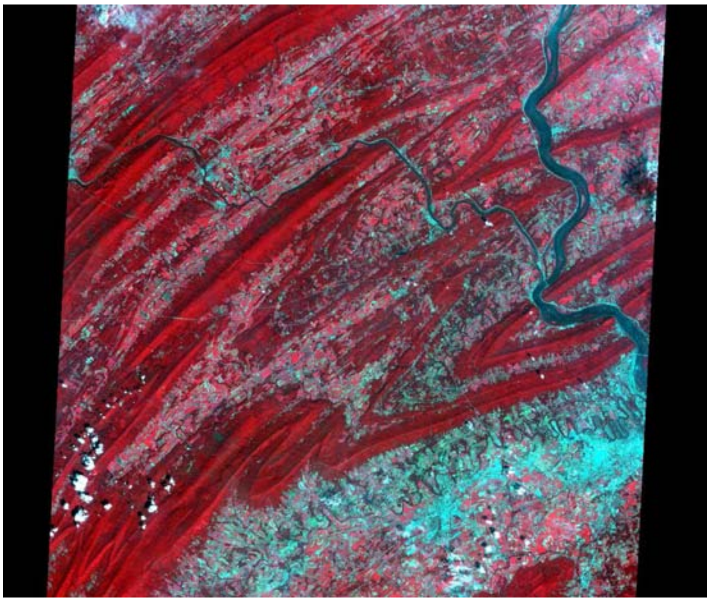

Specific terrain features, which are characterized by different resistance of erosion, are visible.

Fold structures in Pennsylvania, USA (ASTER Visible and Near-infrared image)

The continuous layers and their superposition can be easily recognized in sparse vegetated region.
Visible and near-infrared color composite image with 15 m resolution.

Zagros Mountains, Iran (ASTER image observed on 2004/8/16)

PALSAR image can be used for geologic structure analysis

PALSAR ScanSAR image, which observes wide area, will help the interpretation of regional geologic structure.

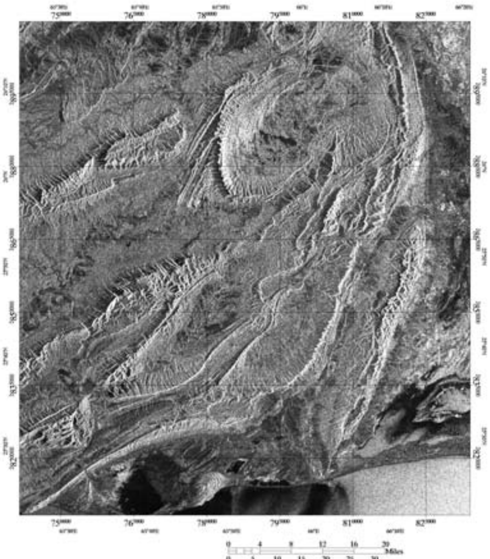

Observed on 2007/02/02

(Published geologic map of 1/2,000,000)

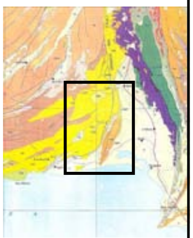

PALSAR ScanSAR image (Southern part of Pakistan) 1:500,000

ASTER DEM will help the analysis of geologic structural features.

ASTER color composite image

Viewing direction and exaggeration can be easily selectable.

3D image, viewing from the South.

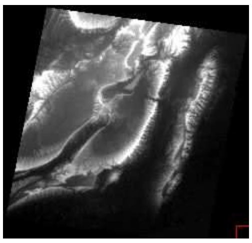

ASTER DEM

3D image, viewing from the North.

observed on 2006/11/11

Visual interpretation by expert, using Landsat satellite imagery

Geologic structure map
of Tohoku region in Japan
Hoshino et al.(1977)

Legend

linear features
fold structures
volcanic structures
geologic units
and boundaries
mineral deposits

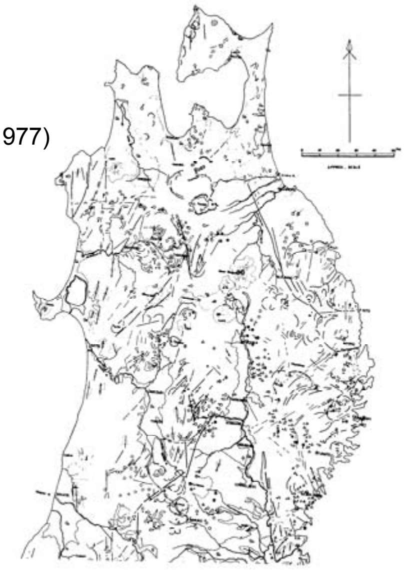

Example of photo-interpretation elements in geology

dendritic | parallel
radial | centripetal
rectangular | trellis
annular | deranged

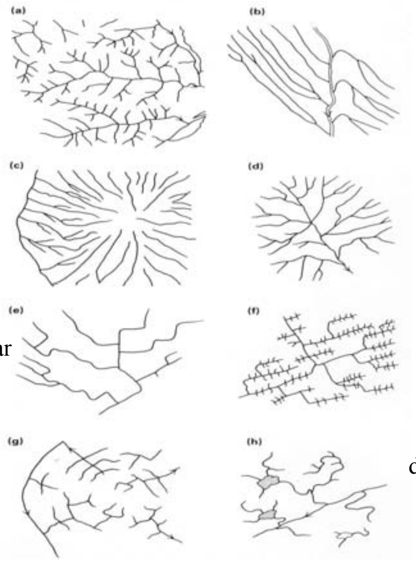

Typical drainage patterns

Silicate rock mapping using ASTER TIR data

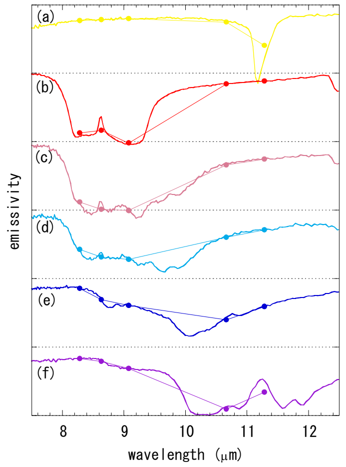

Emissivity spectra of typical terrestrial rocks: a) limestone, b) siliceous rock (quartzite), c) felsic rock (granite), d) intermediate rock (quartz diorite), e) mafic rock (gabbro), f) ultramafic rock (peridotite).

(by Y. Ninomiya)

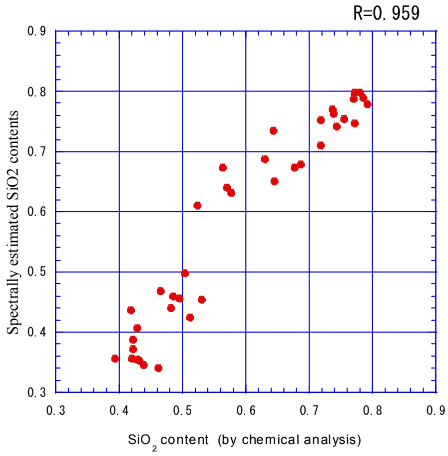

The relationship between the chemically determined SiO2 contents and the spectrally estimated ones. (by Y. Ninomiya)

Defining lithologic indices for ASTER-TIR
(Ninomiya and Fu, 2002)

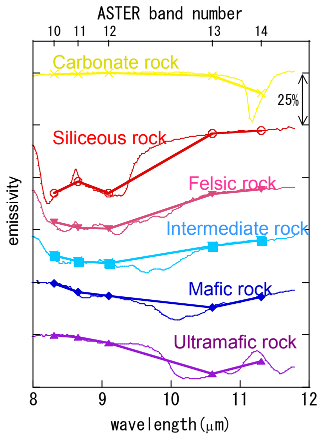

Carbonate Index $CI = \frac{D_{13}}{D_{14}}$.

Quartz Index $QI = \frac{D_{11} \times D_{11}}{D_{10} \times D_{12}}$.

(Mafic Index $MI_{old} = \frac{D_{12}}{D_{13}}$)

Improved **Mafic Index**

$$MI = \frac{MI}{CI^3}$$

Siliceous rock: usually sedimentary, relatively high quartz content with low feldspars content rock.

AIST

Geological mapping in China, using ASTER data

Calcite Index Carbonate Index SiO_2 Content

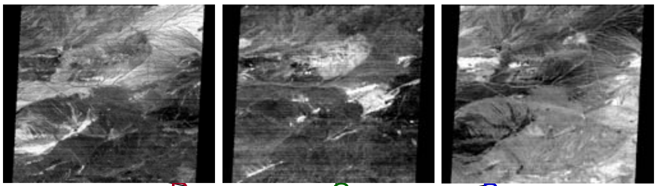

（Research area：
The Beishan mountain, Gansu Province, China）

R G B

Color composite

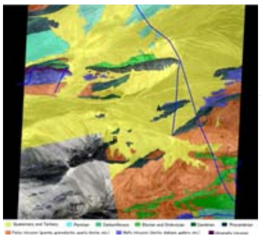

Comparison

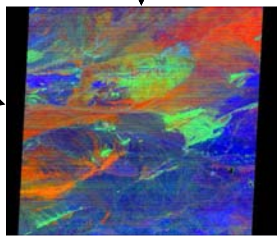

Geologic Map
（Combined with ASTER VNIR image）

NATIONAL INSTITUTE OF ADVANCED INDUSTRIAL SCIENCE AND TECHNOLOGY (AIST)

AIST

ASTER is always monitoring selected active volcanoes in the world regularly.

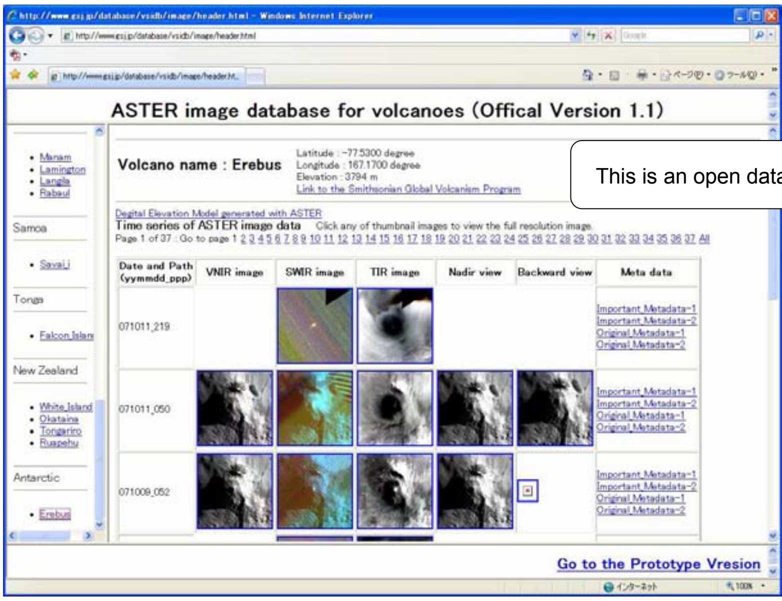

This is an open database.

NATIONAL INSTITUTE OF ADVANCED INDUSTRIAL SCIENCE AND TECHNOLOGY (AIST)

ASTER DSM data is also provided.

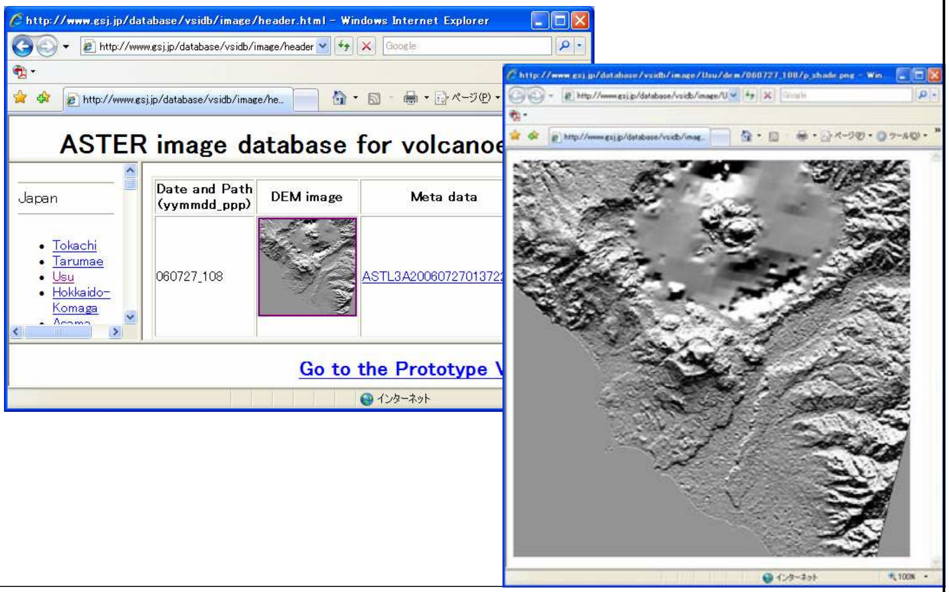

Sulfur dioxide flux monitoring using ASTER TIR data

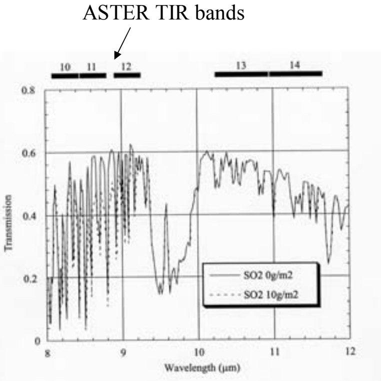

Atmospheric transmission spectrum calculated with/without sulfur dioxide in the thermal region

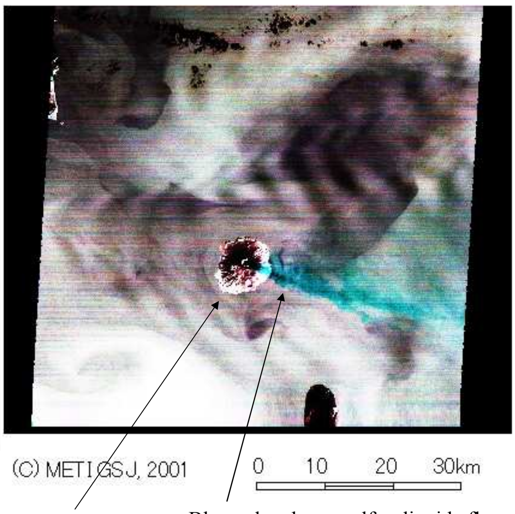

Miyake-jima island

Blue color shows sulfur dioxide flux emitted from the crater

ASTER shows lava flow at the summit of Mt. Merapi, Java island, Indonesia.

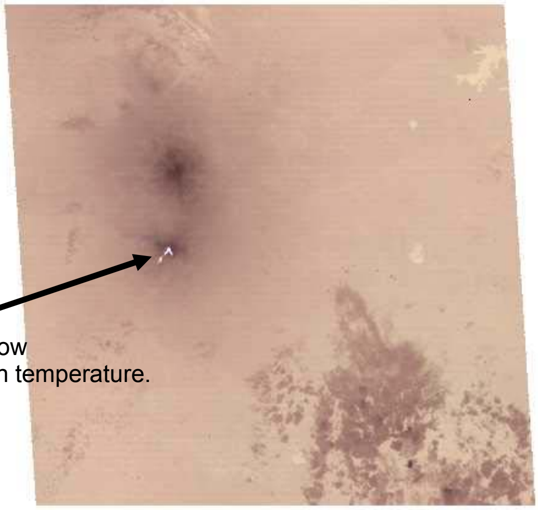

ASTER TIR image (acquired at night on 2006/05/30)

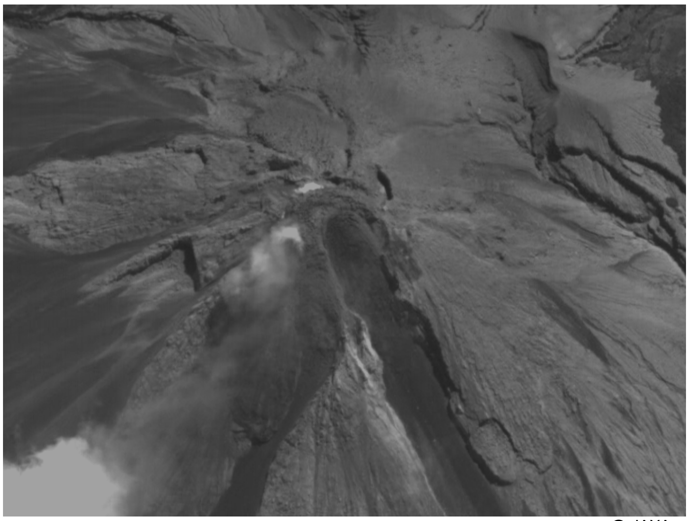

@ JAXA

PRISM image with high spatial resolution (2.5 meters) shows details of the summit area. Stereo-viewing will help more for volcanic interpretation..

PRISM image (nadir-viewing) of Mt. Merapi, Indonesia

Observation date is 2006/09/12.

Image enhancement (left: original, right: enhanced)

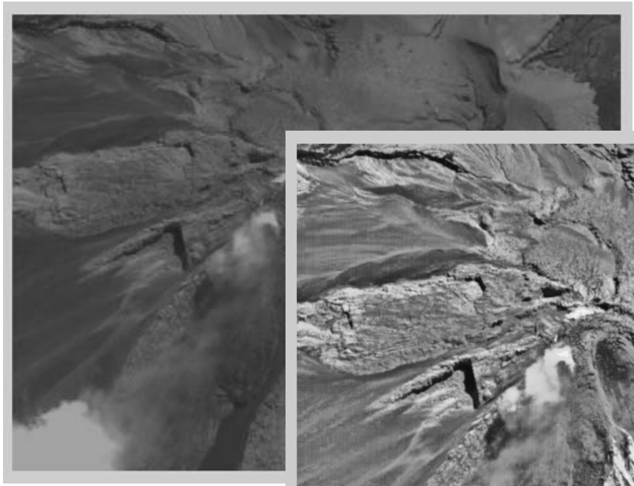

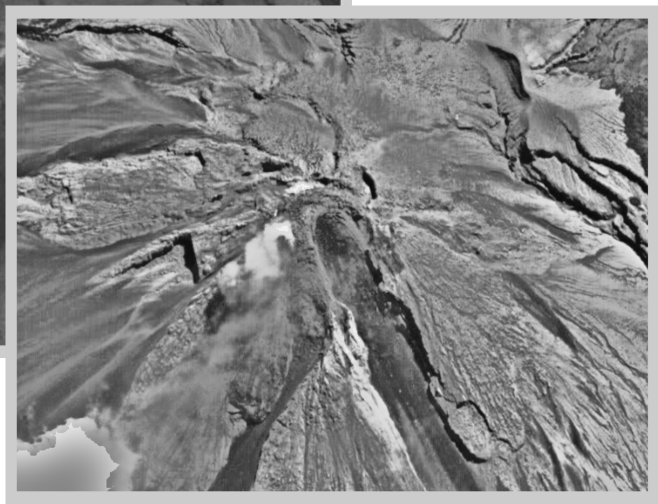

enhanced

original

EO-1/Hyperion

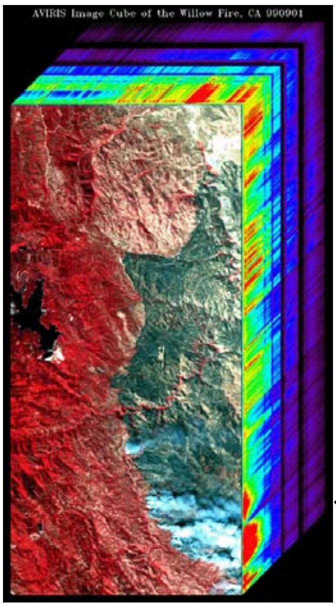

Data concept of Hyperspectral Imager

Wavelength
(224 channels of AVIRIS)

Courtesy of NASA

Hyperspectral data is often called as 'image cube'.

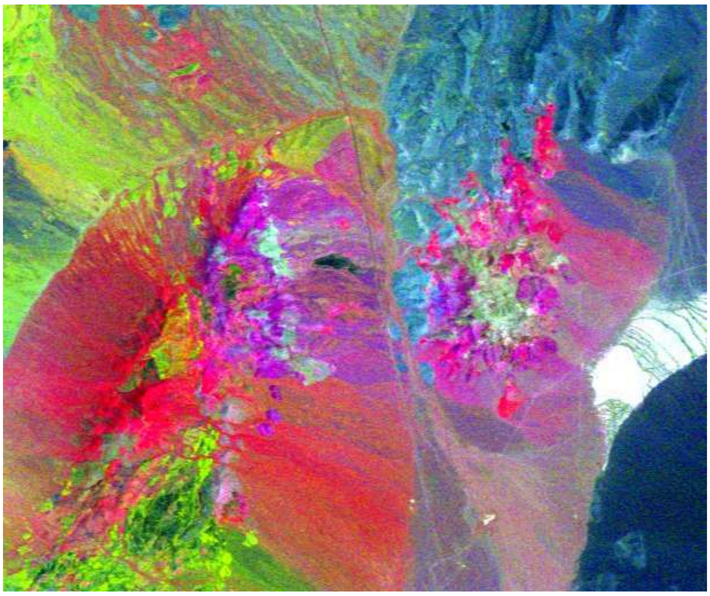

Cuprite, NV. USA

Decorrelation stretch image of AVIRIS data (183 band, 193 band, 207 band)

Spectral reflectance of clay minerals

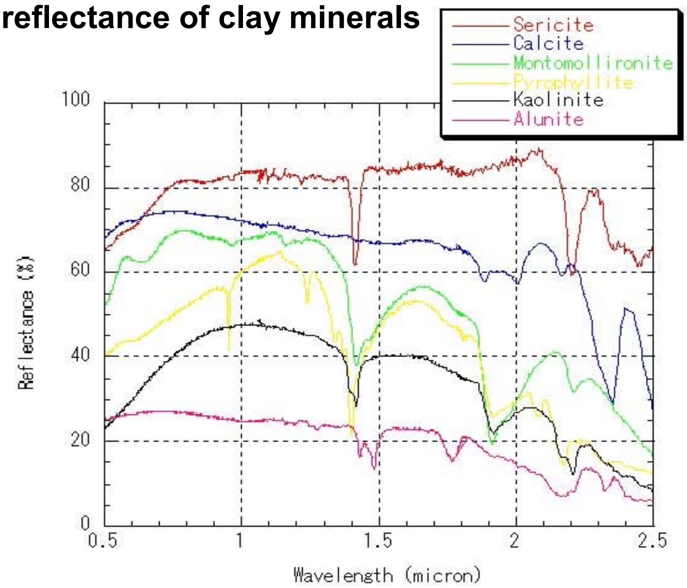

AIST

Spectra library is useful data for analysis

Reflectance values are shifted for visual purpose.

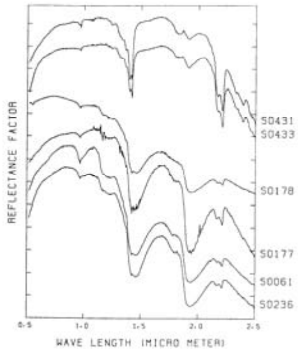

Sample number

sam.Sample_ID	!sam.Site	!lab.Measurement_ID!	norm.Kaolinite
KGa-1	!Washington County	!S0431 !	90.92000
KGa-2	!Warren County	!S0433 !	90.58000
860819F2	!Goshogake	!S0178 !	71.25000
860819F1	!Fukenoyu	!S0177 !	70.59000
851021-T1	!Goshogake	!S0061 !	64.00000
870216-S6	!Komatsu-jigoku	!S0236 !	62.46000

Example of AIST's spectra library (Kaolinite)

AIST

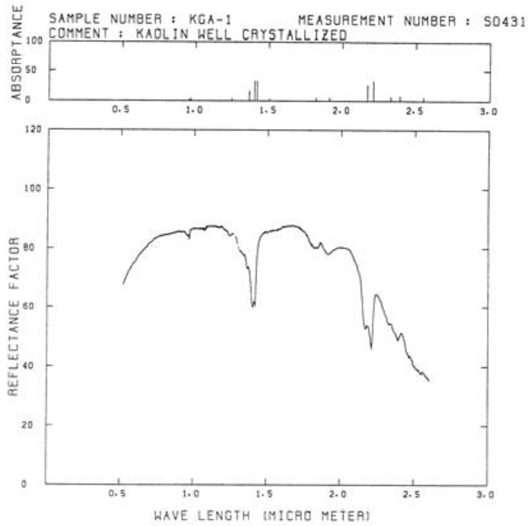

ABSORPTION NO.	WVL.	ABS.
1	2.212	31.9
2	1.402	31.8
3	1.419	31.6
4	2.171	25.9
5	1.366	16.6
6	2.391	8.7
7	2.330	7.0
8	2.552	6.4
9	1.911	5.8
10	1.822	5.6
11	1.248	4.0
12	0.969	4.0
13	1.503	2.8
14	0.958	2.5

Spectra library at AIST (continued)
This figure shows absorbed wavelength and absorption depth of kaolinite.

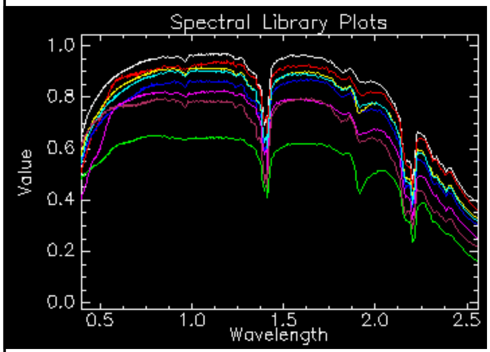

Spectra of various kaolinite minerals (using USGS's SpecLab data)

Spectra of various allunite minerals

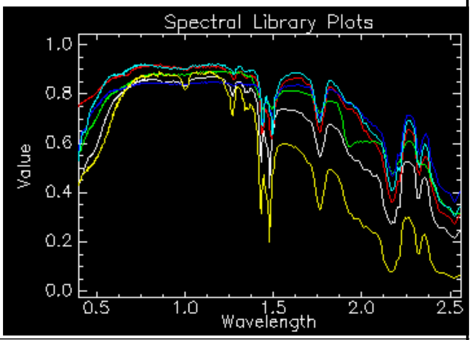

You can see similar reflectance pattern for both minerals with different level.

Reflectance spectra measurement in the field

Possible to measure in visible and near-infrared (0.4～2.5μm) region

GER's Field Spectrometer

After reflectance conversion

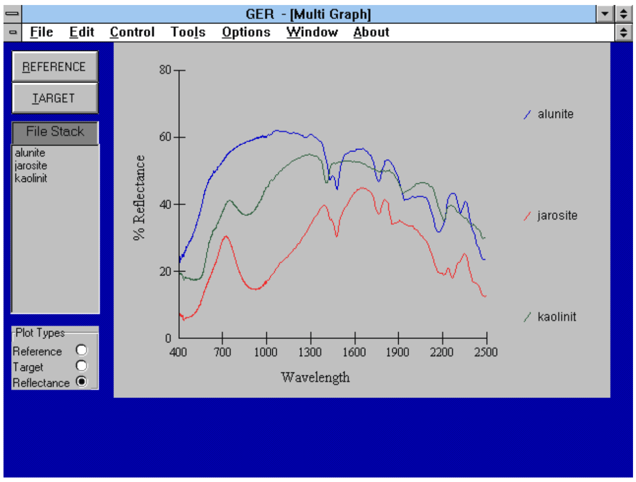

from GER's site (http://www.ger.com)

AIST

Satellite-borne SAR

Polarization mode

1) L-band SAR

SEASAT/SAR (1978)
JERS-1/SAR (1992-1998) HH
(ALOS/PALSAR) (2005-) HH+HV+VH+VV

2) C-band SAR

ERS-1/AMI (1991-) } VV
ERS-2/AMI (1995-) }
RADARSAT-1/SAR (1995-) HH
ENVISAT/ASAR (2002-) HH+VV
(RADARSAT-2/SAR)

For airborne SAR, various kinds of frequency (Ku, X, C, L, P) and polarization are utilized to observe the Earth's surface. For example, CV-580 (Canada/CCRS), AIRSAR (US/JPL), Pi-SAR (Japan/JAXA, NICT), ERR SAR (China), and others.

AIST

Repeat-pass interferometry for Satellite SAR system

Observation geometry

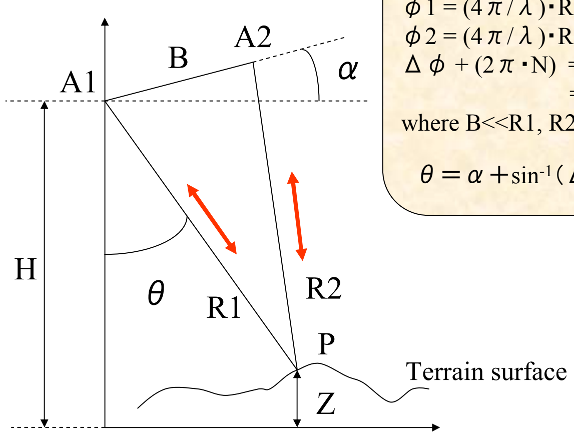

Basic equations

$$Z = H - R1 \cdot \cos\theta \cdots (1)$$
$$\phi 1 = (4\pi/\lambda) \cdot R1$$
$$\phi 2 = (4\pi/\lambda) \cdot R2$$
$$\Delta\phi + (2\pi \cdot N) = \phi 2 - \phi 1 = (4\pi/\lambda) \cdot (R2 - R1) = (4\pi/\lambda) \cdot B \cdot \sin(\theta - \alpha) \cdots (2)$$

where $B \ll R1, R2$

$$\theta = \alpha + \sin^{-1}(\Delta\phi \cdot \lambda / 4\pi / B)$$

Right part can be derived using observed data.

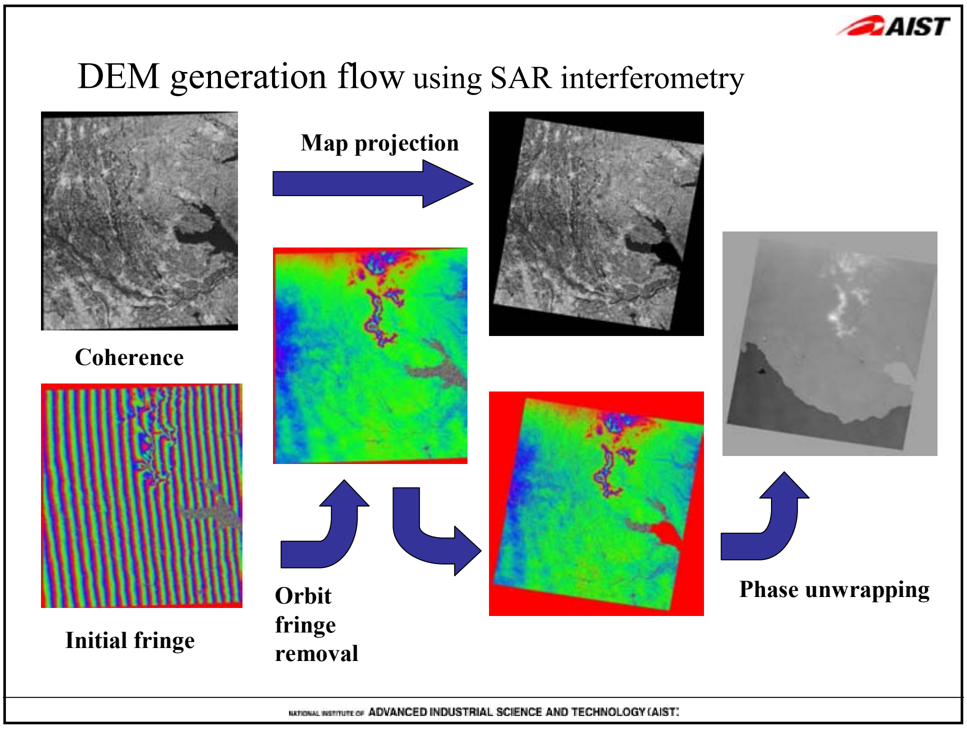
AIST
DEM generation flow using SAR interferometry
Map projection
Coherence
Initial fringe
Orbit
fringe
removal
Phase unwrapping
NATIONAL INSTITUTE OF ADVANCED INDUSTRIAL SCIENCE AND TECHNOLOGY (AIST)

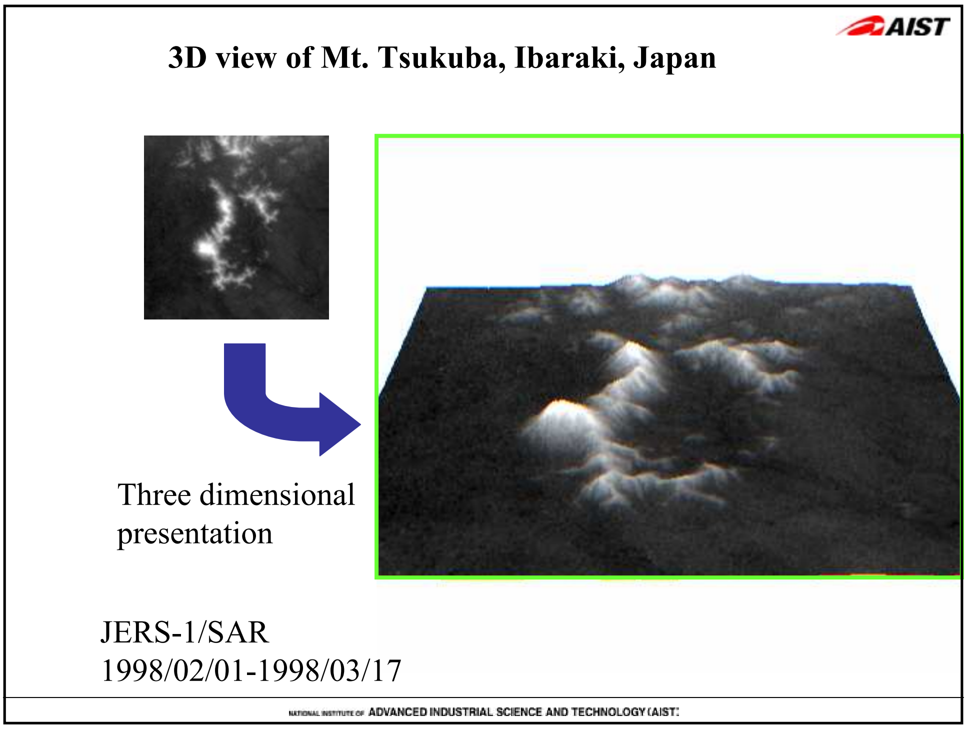
AIST
3D view of Mt. Tsukuba, Ibaraki, Japan
Three dimensional
presentation
JERS-1/SAR
1998/02/01-1998/03/17
NATIONAL INSTITUTE OF ADVANCED INDUSTRIAL SCIENCE AND TECHNOLOGY (AIST)

Processing flow for land deformation mapping (DInSAR)

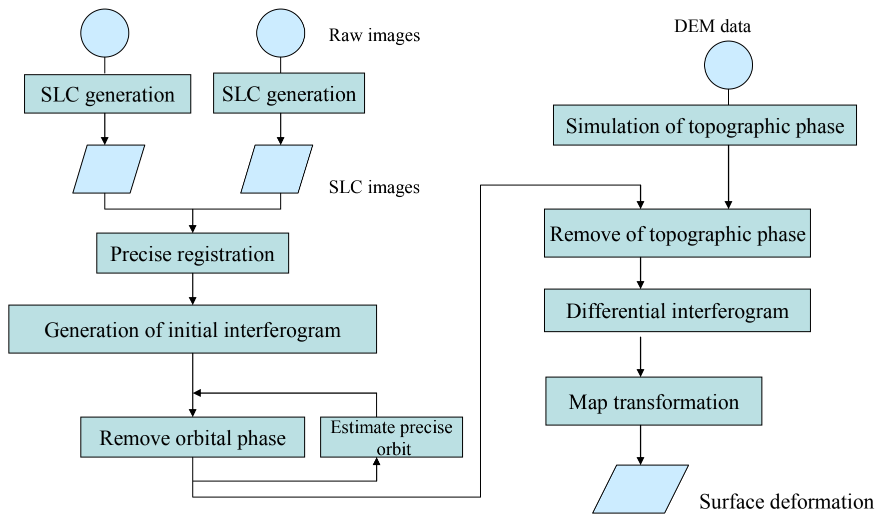

NOTE : SLC means Single Look Complex.

Ground deformation by earthquake is visualized by InSAR

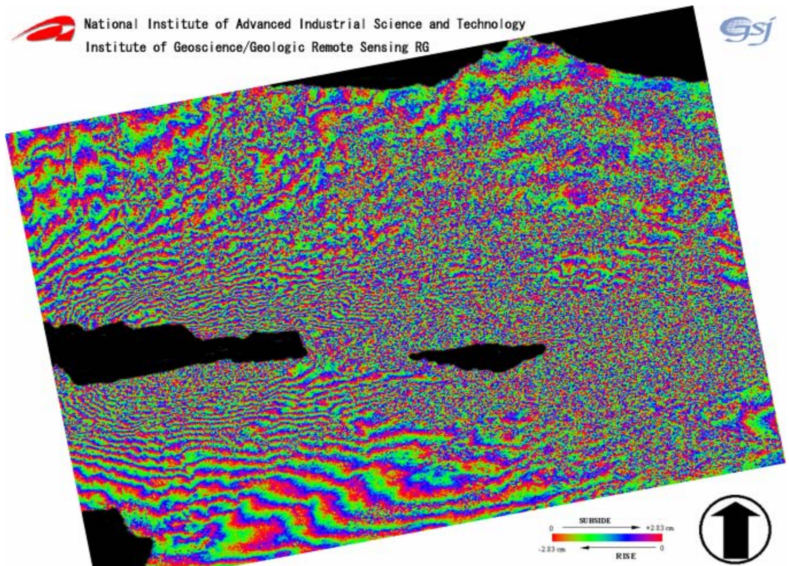

Land deformation after Izmit earthquake in Turkey,1999

Northern Kanto Area (1993/02/24-1996/11/19)
The Red>Yellow>Blue color change shows subsidence in land.

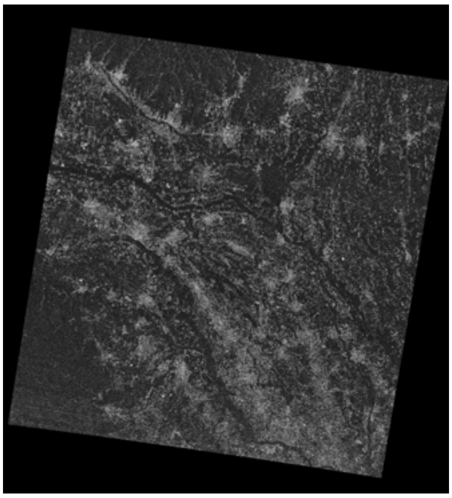

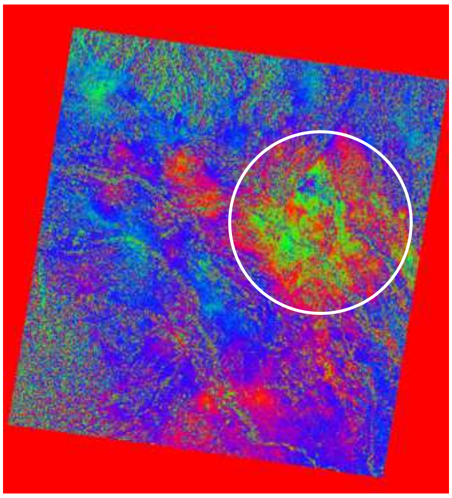

Bp=-170 m

50 m mesh GSI's DEM is used.

Example : **Western Jakarta / Indonesia**

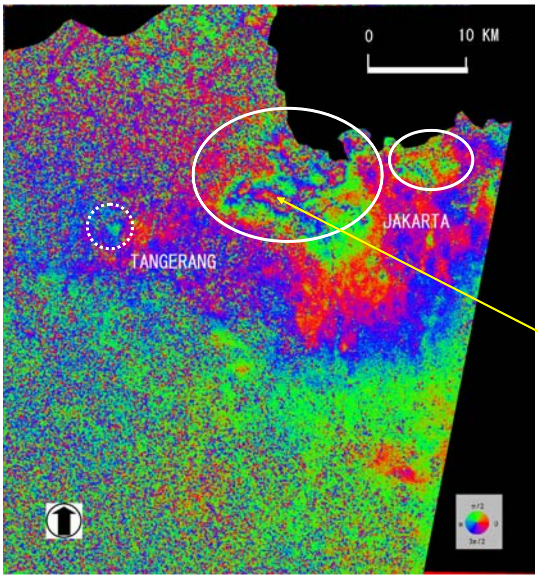

Well known subsided area

JERS-1/SAR (1996/01/17 - 1998/03/19)

AIST

Land subsidence mapping in China

Chang Jiang (Yangtze)

Coherence

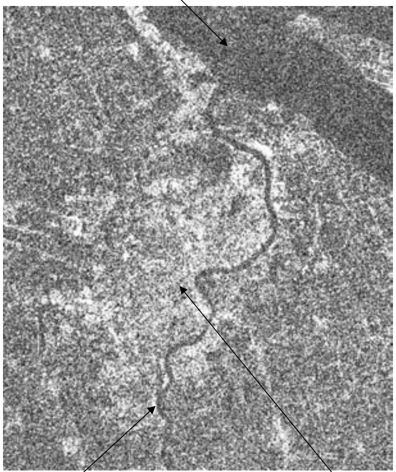

Subsided regions

Phase

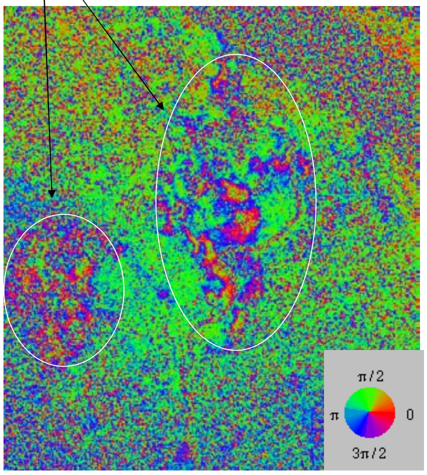

During 1995/03/01-1998/01/20

Huangpu Jiang

Shanghai city and its suburbs

One color cycle shows approx. 12 cm deformation in the slant range.

JERS-1/SAR

NATIONAL INSTITUTE OF ADVANCED INDUSTRIAL SCIENCE AND TECHNOLOGY (AIST)

AIST

Overview of Airborne Synthetic Aperture Radar (Pi-SAR)

Pi-SAR consists of X-band and L-band SAR systems.

X-band (frequency: 9.55GHz, wavelength: approx. 3cm)
L-band (frequency: 1.27GHz, wavelength: approx. 24cm) from http://www.das.co.jp
from http://www2.nict.go.jp/dk/c215/index.html

NATIONAL INSTITUTE OF ADVANCED INDUSTRIAL SCIENCE AND TECHNOLOGY (AIST)

Pi-SAR L-band color composite (RGB=HH,HV,VV) sample image

Osaka city

Observed on 2003/05/03

L-band (frequency: 1.27GHz, wavelength: 24cm)

from http://www.eorc.jaxa.jp

Polarization analysis of SIRC data (Vegetation and Sand)

Parallel polarization

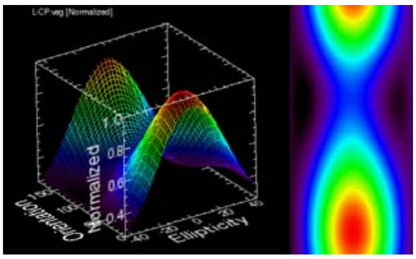

Parallel polarization

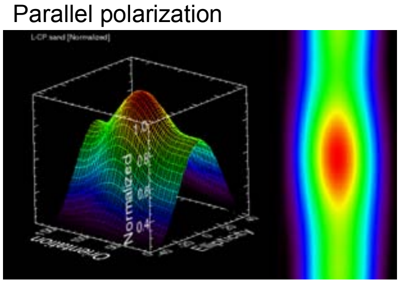

Cross polarization

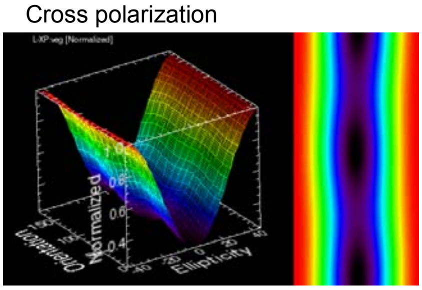

Cross polarization

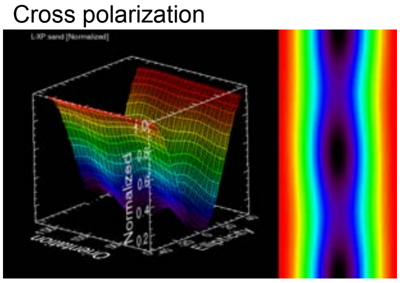

(a) vegetation

(b) sand

AIST

Classification example using PALSAR polarimetric data

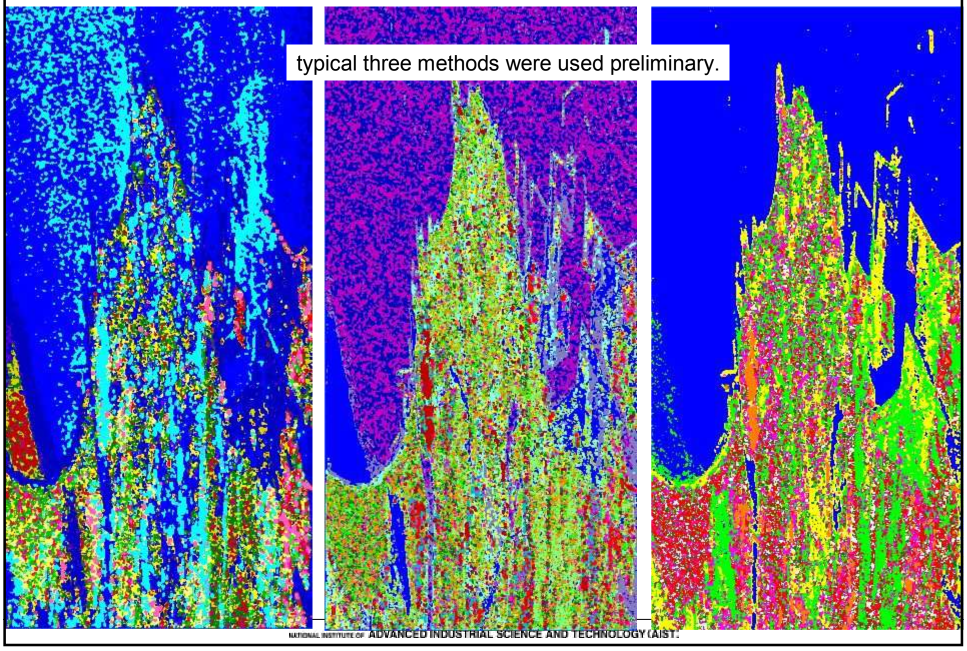

NATIONAL INSTITUTE OF ADVANCED INDUSTRIAL SCIENCE AND TECHNOLOGY (AIST)

AIST

Available tools for image processing and analysis

Simple image handling is possible using PC.

- GIMP
- HyperCube (US Army) and MicroMSI (DMA/USA)
  - possible to handle hyperspectral data
- MultiSpec
  - famous image processing freeware
- many other freewares are available now.

Image viewers: there are many freeware, such as Freelook, ENVIview, others.

NATIONAL INSTITUTE OF ADVANCED INDUSTRIAL SCIENCE AND TECHNOLOGY (AIST)

AIST

I hope this will help you to use and interpret remotely sensed imageries for your interested applications.

Thanks !

NATIONAL INSTITUTE OF ADVANCED INDUSTRIAL SCIENCE AND TECHNOLOGY (AIST)